Hydraulic Control of Three-Layer Exchange Flows: Application to the Bab al Mandab

DAVID A. SMEED

James Rennell Division for Ocean Circulation and Climate, Southampton Oceanography Centre, Southampton, United Kingdom

(Manuscript received 20 January 1998, in final form 30 November 1999)

ABSTRACT

Two-layer hydraulic models have proven to be extremely useful in understanding a number of exchange flows through straits, for example, the Strait of Gibraltar. There are, though, some strait flows that cannot be represented by a two-layer model. A very striking example is the Bab al Mandab. In the exchange between the Red Sea and the Gulf of Aden, three distinct water masses are observed in the strait during summer. The wintertime flow is, though, very different, with only two layers observed in the strait.

In this paper a three-layer model of hydraulically controlled exchange flows is described The model can represent exchange flows that are controlled with respect to either the first or second (or both) internal modes. A number of different examples are discussed.

The model is able to explain the qualitative features of the seasonal variation of the flow in the Bab al Mandab. In particular, the reversal of the direction of flow of the surface layer and the intrusion into the Red Sea of cold intermediate water from the Gulf of Aden during the summer months can be explained by upwelling in the Gulf of Aden forced by the southwest monsoon.

1. Introduction

The deep basins of the world's oceans are separated by ridges, and much of the exchange between basins occurs as flow through gaps or over sills. Thus, these topographic features have a considerable impact on the large-scale thermohaline circulation of the deep oceans. Similar processes determine exchanges with marginal seas. The Mediterranean, the Red Sea, and the Arabian Gulf are all important sources saline water. Each of them is connected to the global ocean via a narrow and shallow strait.

Much progress in understanding these flows has been made using hydraulic models. Based on the shallow water equations, these models make a number of additional assumptions. Following the work of Armi (1986) a number of authors (Armi and Farmer 1986; Farmer and Armi 1986; Dalziel 1991) examined the case of two homogeneous layers flowing through channels of rectangular cross section. This work gave much insight into geophysical flows such as the exchange through the Strait of Gibraltar, a case to which much attention has been given (e.g., Farmer and Armi 1988; Bryden and Kinder 1991; Bryden et al. 1994). However, these models neglected a number of physical processes and a number of papers have followed examining the effects of nonrectangular cross section (Bormans and Garrett 1989; Dalziel 1992), rotation (Dalziel 1990; Pratt and Lundberg 1991), dissipation (Bormans and Garrett 1989), and recently, time dependent forcing (Helfrich 1995).

Surprisingly few authors have addressed the problem of more complex stratification in the context of hydraulic control. However, there are a number of related stratified flows that have been investigated. These include the unidirectional flow of a stratified fluid over an obstacle with an imposed upstream velocity (see, e.g., Baines 1987, 1988, 1995; Denton 1990) and the response of a stratified reservoir to the withdrawal of fluid by a localized sink (Imberger and Patterson 1990). Killworth (1992) considered, theoretically, the case of a continuously stratified flow over a sill, and Armi and Williams (1993) examined experimentally the flow of a stratified fluid through a contraction. Hogg (1983), who also included the effects of rotation, demonstrated how a flow may be controlled with respect to the slowest mode in a three-layer model of the Vema channel. These are essentially forced problems with unidirectional flow, and are distinct from exchange flow (i.e., with flow in both directions) that results from a set of basically static reservoir conditions.

Multilayer exchange flows have been considered by

Corresponding author address: Dr. David A. Smeed, James Rennell Division for Ocean Circulation and Climate, Southampton Oceanography Centre, Empress Dock, Southampton SO14 3ZH, United Kingdom.
E-mail: d.a.smeed@soc.soton.ac.uk

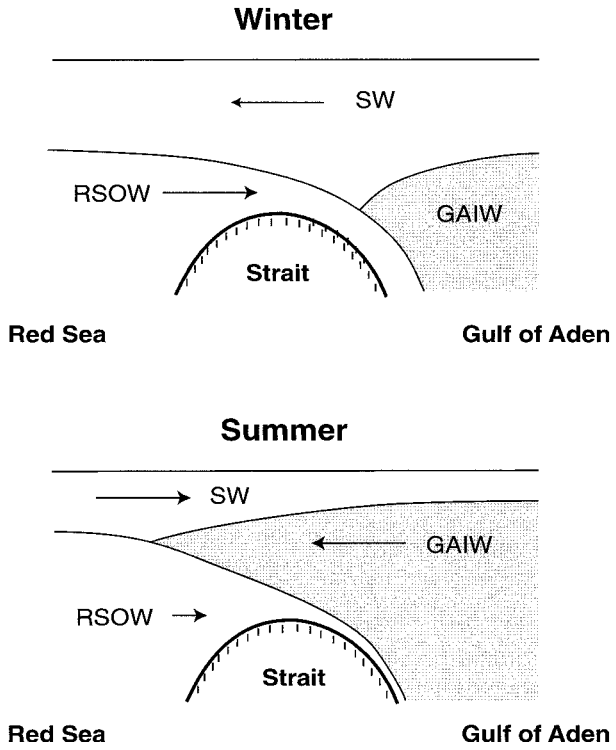

FIG. 1. Sketch of the two circulation patterns in the Bab al Mandab: (a) winter and (b) summer. Here, SW = surface water, GAIW = Gulf of Aden intermediate water, and RSOW = Red Sea outflow water.

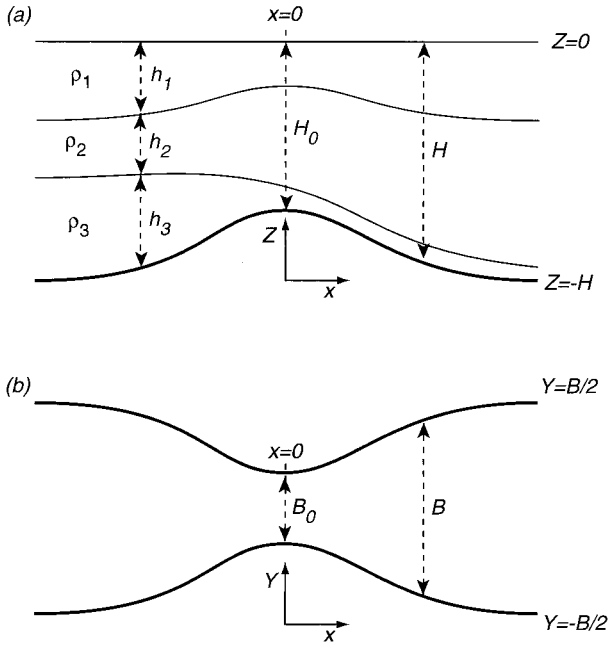

FIG. 2. Model configuration: (a) x–Y plane and (b) x–Z plane. The flow is composed of three homogeneous layers each of density ρ_i and depth h_i. There is a coincident sill and narrows at $x = 0$.

Engqvist (1996). The flows studied by Engqvist were restricted to those for which one of the layers had zero flux. In this case the opposing flows above and below the layer of no motion are decoupled. The flows considered by Engqvist (1996) were controlled with respect to the fastest internal wave mode. The work described in this paper complements that of Engqvist, although only three layers are represented, a wider class of exchange flows are permitted in which the fastest mode may be subcritical everywhere.

A very striking example of exchange flow for which two-layer models are inadequate is the Bab al Mandab (Smeed 1997; Murray and Johns 1997; Pratt et al. 1999, 2000). Three distinct water masses are observed in the strait. During the winter, surface water flows in to the Red Sea above dense salty water flowing out into the Gulf of Aden. At the exit of the strait in the Gulf of Aden a third water mass of intermediate density is observed. During the summer monsoon, upwelling lifts the interface between the intermediate water and the surface water in the Gulf of Aden to within 20 m of the surface and intermediate water flows in to the Red Sea. The direction of flow of surface water is reversed so that it flows into the Gulf of Aden, and the outflow of dense water from the Red Sea is reduced to 10%–15% of the wintertime flux (Maillard and Soliman 1986). The summer and winter flows are illustrated schematically in Fig. 1.

It is often suggested that the reversal in the flow of the surface layer is a direct consequence of the reversal of the surface winds in the strait (e.g., Maillard and Soliman 1986). Indeed there are strong correlations between the local winds and the fluxes through the strait (Murray and Johns 1997). However, Patzert (1974) has suggested that the dominant effect is the upwelling of the intermediate waters in the Gulf of Aden. Smeed (1997) examined the problem again and also considered that the upwelling in the Gulf of Aden was the primary mechanism for the change in the circulation pattern of the strait. To examine the question in more detail a model of three-layer exchange flows has been developed. The model is described in the sections 2 and 3 of this paper and its application to the Bab al Mandab is discussed in section 4.

While the application to the Bab al Mandab is the primary focus of this paper, the theory is applicable to other straits and gives insight into the problem of control of continuously stratified flows.

2. The three-layer model

The development of the following equations is similar to that in previous studies of two-layer exchange (e.g., Dalziel 1991). In particular, the configuration is one of two large reservoirs connected by a channel, of rectangular cross section, whose width and depth vary on scales that are long compared to the channel width so that the flow may considered to be unidirectional. The fluid is assumed to be Boussinesq, hydrostatic, inviscid,

and steady. The flow is composed of three immiscible layers as sketched in Fig. 2.

The momentum equations in each of the layers are

$$\frac{\partial}{\partial x}\left(\frac{1}{2}u_1^2 + \frac{p_0}{\overline{\rho}}\right) = 0, \quad (1)$$

$$\frac{\partial}{\partial x}\left(\frac{1}{2}u_2^2 + \frac{p_0}{\overline{\rho}} - g_1' h_1\right) = 0, \quad (2)$$

$$\frac{\partial}{\partial x}\left[\frac{1}{2}u_3^2 + \frac{p_0}{\overline{\rho}} - g_1' h_1 - g_2'(h_1 + h_2)\right] = 0, \quad (3)$$

where p_0 is the pressure at the surface of the upper layer, u_i is the along channel velocity, h_i the thickness, and ρ_i the density of the ith layer. The reduced gravity $g_i' = 2g(\rho_{i+1} - \rho_i)/\overline{\rho}$, $i = 1, 2$, and $\overline{\rho}$ is the mean density.

The continuity equation for each layer is

$$\frac{\partial}{\partial x}(u_i a_i) = 0 \qquad i = 1, 3, \quad (4)$$

where $a_i = Bh_i$, and $B(x)$ is the width of the channel. The total depth of the channel is $H(x) = h_1 + h_2 + h_3$. Two Bernoulli equations are obtained by taking the differences of the integrals of Eqs. (1)–(3):

$$\frac{1}{2}u_1^2 - \frac{1}{2}u_2^2 + g_1' h_1 = H_1', \quad (5)$$

$$\frac{1}{2}u_2^2 - \frac{1}{2}u_3^2 + g_2'(h_1 + h_2) = H_2', \quad (6)$$

where H_1' and H_2' are constants. The continuity equation (4) implies that the flux in each layer is a constant, Q_i, that is,

$$u_i a_i = Q_i \qquad i = 1, 3. \quad (7)$$

Substituting for the u_i the Bernoulli equations [(5) and (6)] may be written

$$\frac{1}{2B^2}\left(\frac{Q_1^2}{h_1^2} - \frac{Q_2^2}{h_2^2}\right) + g_1' h_1 = H_1', \quad (8)$$

$$\frac{1}{2B^2}\left(\frac{Q_2^2}{h_2^2} - \frac{Q_3^2}{h_3^2}\right) + g_1'(h_1 + h_2) = H_2'. \quad (9)$$

The equations are nondimensionalized using B_0 and H_0, the minimum values of the channel width and depth, and $g' = g_1' + g_2'$ as follows:

$$\begin{aligned} B &= B_0 b, & H &= H_0 h, & g_1' &= r g', \\ g_2' &= (1 - r)g', & h_1 &= H_0 h y, & & \\ h_2 &= H_0 h(1 - y - z), & h_3 &= H_0 h z, & & \\ H_j' &= g' H_0 H_j, & j &= 1, 2, & & \\ Q_i &= B_0 H_0 (g' H_0)^{1/2} q_i, & i &= 1, 3. & & \end{aligned} \quad (10)$$

The parameter $r = (\rho_2 - \rho_1)/(\rho_3 - \rho_1)$ can vary between 0 and 1. Thus $h(x)$ and $b(x)$ are the non-dimensional depth and width of the channel, and $y(x)$ and $z(x)$ are the non-dimensional depths of the upper and lower layers. The nondimensional depth of the middle layer is $1 - y - z$.

The nondimensional Bernoulli equations are

$$J = \frac{1}{2h^2 b^2}\left[\frac{q_1^2}{y^2} - \frac{q_2^2}{(1 - y - z)^2}\right] + rhy - H_1 = 0, \quad (11)$$

$$K = \frac{1}{2h^2 b^2}\left[\frac{q_2^2}{(1 - y - z)^2} - \frac{q_3^2}{z^2}\right] + (1 - r)h(1 - z) - H_2 = 0. \quad (12)$$

Summing (11) and (12) gives

$$L = \frac{1}{2h^2 b^2}\left(\frac{q_1^2}{y^2} - \frac{q_3^2}{z^2}\right) + rhy + (1 - r)h(1 - z) - H_1 - H_2 = 0. \quad (13)$$

Only two of (11, 12 and 13) are independent, but it is sometimes convenient to use different pairs of these equations. Note, for example, that when the middle layer has zero thickness, then substituting $y + z = 1$ into Eq. (13) the equation for two-layer flow is obtained.

Following Gill (1977) for single layer flows, and Dalziel (1991) for two-layer flows, J and K can be regarded as functionals. Thus we are seeking solutions to

$$\mathbf{J}(b, h, q_1, q_2, q_3, H_1, H_2; y, z) = \begin{pmatrix} J \\ K \end{pmatrix} = 0. \quad (14)$$

Solutions of (14) can be traced along the channel by solving

$$\begin{pmatrix} \dfrac{dJ}{dx} \\ \dfrac{dK}{dx} \end{pmatrix} = \begin{pmatrix} 0 \\ 0 \end{pmatrix}, \quad (15)$$

which can be written as

$$\mathbf{M}\begin{pmatrix} \dfrac{\partial y}{\partial x} \\ \dfrac{\partial z}{\partial x} \end{pmatrix} = -\begin{pmatrix} \dfrac{\partial J}{\partial x} \\ \dfrac{\partial K}{\partial x} \end{pmatrix} = \mathbf{N}\begin{pmatrix} \dfrac{\partial b}{\partial x} \\ \dfrac{\partial h}{\partial x} \end{pmatrix}, \quad (16)$$

where

$$\mathbf{M} = \begin{pmatrix} \dfrac{\partial J}{\partial y} & \dfrac{\partial J}{\partial z} \\ \dfrac{\partial K}{\partial y} & \dfrac{\partial K}{\partial z} \end{pmatrix}, \quad \text{and} \quad \mathbf{N} = \begin{pmatrix} \dfrac{\partial J}{\partial b} & \dfrac{\partial J}{\partial h} \\ \dfrac{\partial K}{\partial b} & \dfrac{\partial K}{\partial h} \end{pmatrix}. \quad (17)$$

Froude numbers for each layer can be defined as follows:

$$F_1^2 = \frac{u_1^2}{g'h_1} = \frac{q_1^2}{b^2h^3y^3},$$

$$F_2^2 = \frac{u_2^2}{g'h_2} = \frac{q_2^2}{b^2h^3(1-y-z)^3},$$

$$F_3^2 = \frac{u_3^2}{g'h_3} = \frac{q_3^2}{b^2h^3z^3}, \tag{18}$$

so the terms in the matrix **M** can be expressed as

$$\frac{\partial J}{\partial y} = h(r - F_1^2 - F_2^2),$$

$$\frac{\partial J}{\partial z} = -\frac{\partial K}{\partial y} = -hF_2^2, \quad \text{and}$$

$$\frac{\partial K}{\partial z} = h(F_3^2 + F_2^2 - 1 + r). \tag{19}$$

a. Controlled flows

Control of two-layer flows has been discussed by Armi (1986), Dalziel (1991), and others. In a two-layer flow with a rigid lid, there is one internal wave mode. This internal wave mode has two wave speeds associated with it.[1] If the two phase speeds have opposite signs then internal waves can propagate both upstream and downstream and the mode is said to be *subcritical.* If the two phase speeds have the same sign then the internal waves of that mode can propagate in one direction only, and the mode is said to be *supercritical.* When one of the phase speeds is equal to zero then that mode is said to be *critical.* Locations at which the flow are critical are termed *controls.*

In a three-layer flow with a rigid lid there are two possible internal wave modes. In this case each of the two modes may be subcritical, critical, or supercritical. When the flow is critical with respect to one, or both, of the modes

$$\det(\mathbf{M}) = 0 \tag{20}$$

(see, e.g., Baines 1988). Note that

$$\det(\mathbf{M}) = \frac{\partial J}{\partial z}\frac{\partial K}{\partial y} - \frac{\partial J}{\partial y}\frac{\partial K}{\partial z}$$
$$= h^2[F_2^4 - (r - F_1^2 - F_2^2)(1 - r - F_2^2 - F_3^2)]. \tag{21}$$

Equation (20) is analogous to the condition for two-layer flows that the sum of the squares of the two (one for each layer) Froude numbers must be equal to one at a control. In two-layer flows a second condition, that the flow is regular, must also be satisfied at a control (see, e.g., Dalziel 1991).

Conditions for control in multilayered flows have been discussed by Baines (1988), and the case of continuous stratification is considered by Killworth (1992). Two conditions must be satisfied at a control. First, the speed of one of the internal wave modes must vanish [for a three-layer flow this is equivalent to Eq. (20)], and secondly the flow must be regular. The regularity condition can be understood by noting that when (20) holds, then the left hand sides of (16) are not independent and regular solutions are only possible if

$$\frac{\partial K}{\partial y}\frac{\partial J}{\partial x} - \frac{\partial J}{\partial y}\frac{\partial K}{\partial x} = \frac{\partial K}{\partial z}\frac{\partial J}{\partial x} - \frac{\partial J}{\partial z}\frac{\partial K}{\partial x} = 0. \tag{22}$$

Equation (22) is clearly satisfied at a sill where $\partial b/\partial x = \partial h/\partial x = 0$ [from Eq. (16)]. Baines (1988) showed that the flow either side of a sill will be symmetric unless the flow is critical at the sill. However, controls may occur elsewhere and these are referred to as *virtual controls.*

Gill (1977), for single-layer flows, and Dalziel (1991), for two-layer flows, have shown that hydraulically controlled flows can be interpreted as solutions to functional equations, and that controls are the points at which the flow switches from solution branch of the functional to another branch. These ideas can also be applied in the three-layer problem studies here, and indeed different solutions branches of (14) meet when Eqs. (20) and (22) are satisfied.

b. Reservoir conditions

In hydraulic problems the flow is determined by the conditions in the reservoirs either side of the sill. It is therefore interesting to examine the possible flow states in the reservoirs.

Asymptotic solutions of (11) and (12) can be found in the limit of $b \to \infty$. When each of the fluxes q_i is nonzero and $O(1)$ then in the reservoirs, where $b \gg 1$, there are seven possible solutions. The possible reservoir solutions can be labelled as follows: type "i," $i = 1, 3$ is that in which the depth of layer $i \to 0$ as $b \to \infty$, and the other two-layer depths remain O(1); type "$-i$," $i = 1, 3$ is that in which the depth of layer $i \to 1$ as $b \to \infty$ and the other two-layer depths $\to 0$; and the seventh solution, type "0," is that in which all three-layer depths are $O(1)$. Analytic expressions for each of these are given in appendix A, where it is also shown that $\det(\mathbf{M}) < 0$ for type "i," $i = 1, 3$ and >0 for the other solutions. Thus solution type "0" has both modes subcritical, solution types "1," "2," and "3" have one mode subcritical and one mode supercritical, and solution types, "-1," "-2," and "-3" have both modes supercritical.

Examples of solutions in a reservior with $b = \infty$ are illustrated in Fig. 3. The sum of the nondimensional layer depths cannot be greater than one, so all the phys-

[1] In general phase speeds of internal waves are a function of the wavelength. However, we are concerned only with small amplitude long-wavelength waves, as it is these waves that propagate information in the flow.

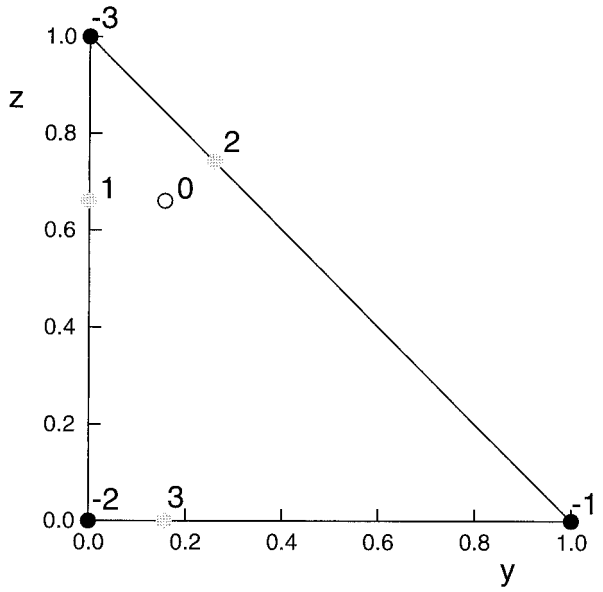

FIG. 3. Solutions to (11) and (12) for an infinitely wide reservoir ($b = \infty$) when there is a nonzero flux in each layer. There are seven different solutions labeled "−3," "−2," "−1," "0," "1," "2," and "3." The open circle represents both modes subcritical, the gray circles represent one mode supercritical, and the black circles represent both modes supercritical. Other parameters are: $H_1 = 0.166$, $H_2 = 0.333$, and $h = 2$.

ically realizable solutions lie in the area bounded by $y = 0$, $z = 0$, and $y + z = 1$.

3. Flow types

To evaluate a solution at some point in the channel we need to know q_1, q_2, q_3, H_1, H_2, and the solution branch at that location. In what follows it is assumed that the total flux $q_B = q_1 + q_2 + q_3$ is imposed. The other four parameters must be determined from the conditions in the reservoirs and the model equations.

If H_1 and H_2 do not have the same values in both reservoirs, at least one hydraulic jump is required to match the flow to the reservoir conditions. At a hydraulic jump there is a transition from supercritical flow to subcritical flow In this paper, the condition that the energy on the supercritical side of the jump be not less than that on the subcritical side is applied. However, a more detailed analysis of hydraulic jumps is beyond the scope of this paper.

Possible flows can be classified according to their upstream[2] and downstream states. In this paper flows are labeled as [*iup, idn*] where *iup* and *idn* refer to the up and downstream states. Note by symmetry that [*idn, iup*] is also a possible flow.

When the upstream and downstream solution types are different then one or more controls are required. At each control there are two equations to be satisfied [(20) and (22)], but we also need to evaluate the location of the control. Thus each control reduces the number of degrees of freedom by one. It is possible for two controls to be coincident.

In the following sections some examples are given. All of these are for the case of flow with equal density differences across the two interfaces (i.e., $r = 0.5$) and no net flow (i.e., $q_B = 0$) in a channel with a coincident sill and narrows at $x = 0$. The types of flow for which examples are given are summarized in Table 1. The examples do not cover all the possible three-layer exchange flow types, but only those which are relevant to the application of the model to the Bab al Mandab. Details of the numerical techniques are given in appendix B.

a. Subcritical flow in both reservoirs

When both modes are subcritical in a reservoir, then both Bernoulli constants are determined by the stratification there. Unless there are one, or more, hydraulic jumps at which the Bernoulli constants can change, the downstream conditions must be the same as those up-

[2] The terms upstream and downstream are used loosely here to mean away from the sill. They are not used to imply a preferred direction.

TABLE 1. Summary of flow types described in the text for which there are no hydraulic jumps. The flows are classified according to the states, either subcritical ("sub"), or supercritical ("sup"), of each of the two internal modes in each of the reservoirs. The column "Figure" refers to the figure in which the flow type highlighted in bold is illustrated.

No. of controls	Flow types	Mode states in reservoirs: Downstream	Mode states in reservoirs: Upstream	No. of reservoir conditions	Degrees of freedom	Figure
0	**[0, 0]**	sub sub	sub sub	2	2	5
1	[0, 1], [0, 2], **[0, 3]**	sub sub	sub sup	2	1	6
2	[0, −1], **[0, −2],** [0, −3]	sub sub	sup sup	2	0	7
2	[1, 2], **[2, 3],** [1, 3]	sub sup	sub sup	2	0	8
3	[1, −1], **[2, −2],** [3, −3]	sub sup	sup sup	1	0	9

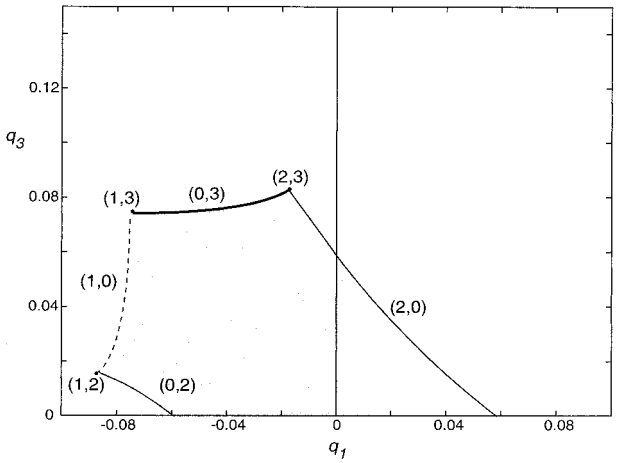

FIG. 4. Solutions in the q_1, q_3 plane. The shaded region denotes the range of fluxes for the case of subcritical flow everywhere (i.e., flow type [0, 0]). The heavy line denotes the range of fluxes for solution type [0, 3], the thin lines denotes flow types [0, 2] and [2, 0], and the dashed line denotes flow type [0, 1]. Flow types [1, 2], [2, 3], and [1, 3] are each only possible at a single point in the half-plane. The Bernoulli constants are $H_1 = 0.166$, $H_2 = 0.333$. Note results for the complete q_1, q_3 plane can be inferred by symmetry about $q_3 = 0$.

stream. In this case there are, usually, no controls.[3] Thus there remain two degrees of freedom, and solutions are possible for a range of fluxes. The boundaries of these areas in the (q_1, q_3) plane[4] can be determined numerically as described in appendix B. The bounding lines have been evaluated for the case in which the depth of the upper two layers in the reservoirs are each ⅓ of the depth of the sill depth. The results are illustrated in Fig. 4. An example of one such flow is given in Fig. 5. Physically, these flows are not very interesting. However, they are a useful starting point for the discussion of the more complex flows below.

If the conditions in the downstream reservoir are perturbed so that one of the Bernoulli constants is different from its upstream value then there must be a hydraulic jump, upstream of the jump the flow will be of the form described in section 3b below. An example of such a flow is illustrated by the broken line in Fig. 6.

b. Both modes subcritical upstream, one mode supercritical downstream

The flows in this category are [0, 1], [0, 3], and [0, 2]. In the upstream reservoir the two interface heights determine the Bernoulli constants. Thus there is only one

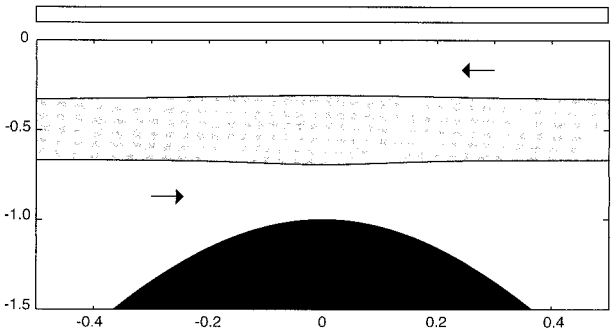

FIG. 5. An example of flow type [0, 0]. The flow is subcritical everywhere (indicated by the white bar across the top of the plot), and there are no controls. Parameters for the solution shown are $H_1 = 0.166$, $H_2 = 0.333$, $q_1 = -0.05$, $q_2 = 0$, and $q_3 = 0.05$. The middle layer is shaded gray, and the arrows indicate the flux in each layer.

value of the downstream interface height for which a solution can be found conserving the Bernoulli function at all points. In this case there is a single control at $x = 0$. There remains one degree of freedom and solution are possible on a line in the (q_1, q_3) plane (see Fig. 4). An example of a flow type [0, 3] is illustrated in Fig. 6.

If the downstream interface height is not the same as the corresponding value upstream there must be at least two controls and one hydraulic jump. Upstream of the hydraulic jump, the solutions will be of the same form as the flows in sections 3c or 3d below.

c. Two modes subcritical upstream, two modes supercritical downstream

The flows in this category are [0, −1], [0, −3], and [0, −2]. For these flows the stratification upstream determines the two Bernoulli constants. When solutions are possible for which the Bernoulli constants remain

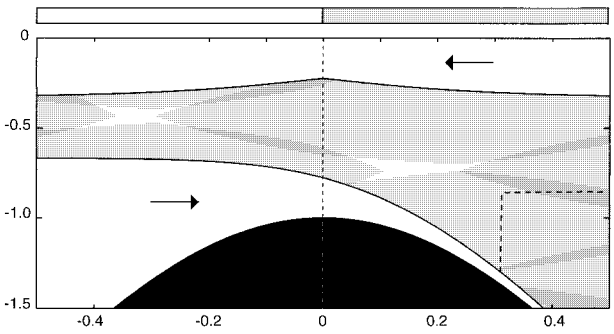

FIG. 6. An example of flow type [0, 3]. The depth of the upper layer is the same up and downstream, and there is a single control at $x = 0$ (indicated by the dashed vertical line). Shading on the bar above the plot indicates where the second mode is supercritical. Parameters for the solution shown are $H_1 = 0.166$, $H_2 = 0.333$, $q_1 = -0.074$, $q_2 = 0$, and $q_3 = 0.074$. The dashed line shows the lower interface for a flow that would be obtained by perturbing the flow in Fig. 5 by decreasing the depth of the lower layer in the downstream reservoir.

[3] An exception is the case of a channel with a flat bottom and a flow in which the layer depths are uniform and $q_1^2/y^2 = q_2^2/(1 - y - z)^2 = q_3^2/z^2$. There can then be an even number of controls located symmetrically about $x = 0$. Such flows are not, however, physically realistic.

[4] Note that $q_2 = -q_1 - q_3$.

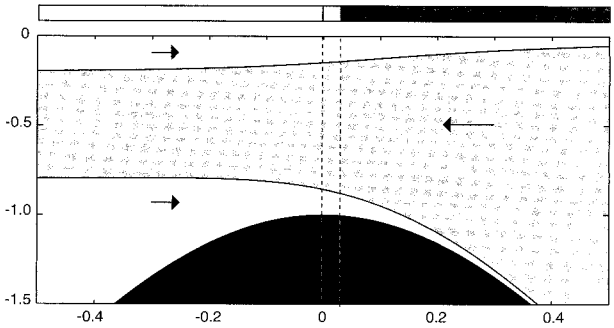

FIG. 7. Solution type [0, −2]. Parameters for the solution shown are $H_1 = 0.2$, $H_2 = 0.8$, $q_1 = 0.037$, $q_2 = -0.074$, and $q_3 = 0.037$. There are two controls (indicated by the dashed vertical lines) at $x = 0$ and at $x = 0.03$. Light shading on the bar above the plot indicates where one mode is supercritical, heavy shading indicates where both modes are supercritical.

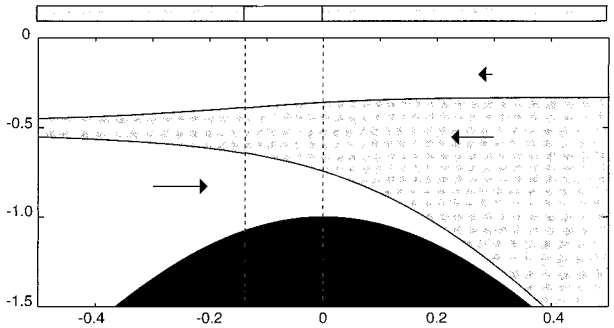

FIG. 8. Solution type [2, 3]. Parameters for the solution shown are $H_1 = 0.166$, H_2, $= 0.333$, $q_1 = -0.017$, $q_2 = -0.066$, and $q_3 = 0.083$. There are two controls (indicated by the dashed vertical lines) one at $x = 0$ and the other at $x = -0.14$. Shading on the bar above the plot indicates where the second mode is supercritical.

unchanged along the channel, there are two controls. One at $x = 0$, the other a virtual control. An example of a flow type [0, −2] is given in Fig. 7.

However, it is not possible to find solutions for all up and downstream conditions. In these cases there must be a hydraulic jump downstream of which the flow is of the type described in section 3e below.

d. One mode supercritical upstream, one mode supercritical downstream

Flows in this category include [1, 2], [3, 2], and [1, 3]. For these three flow types there is one condition upstream and one condition downstream, which determine the two Bernoulli constants. When solutions are possible for which the Bernoulli constants remain unchanged along the channel, there are two controls, one is at $x = 0$ the other is a virtual control. An example of a type [2, 3] flow is shown in Fig. 8.

However, it is not possible to find solutions for all up and downstream conditions. In this case there must be a hydraulic jump upstream of which the flow is of the form discussed in section 3e below.

e. One mode supercritical downstream, two modes supercritical upstream

Flows in this category include [1, −1], [3, −3], and [2, −2]. For these flows there is one condition upstream. Downstream there are no conditions, and one layer occupies almost the whole depth of the channel. For the given upstream condition, the flow in this layer is maximal. There are three transitions and so solutions are possible only for particular values of the fluxes and the Bernoulli constants. An example of a flow type [2, −2] is given in Fig. 9.

4. Application to the Bab al Mandab

The primary objective of this work is to demonstrate that the seasonal variation of the flow in the Bab al Mandab can be explained as a response to the variation in stratification in the Gulf of Aden and the Red Sea. In the preceding sections we have described a model of hydraulically driven exchange flows whose solutions are functions only of the geometry of the strait and the stratification in the reservoirs. In this section the model is used to demonstrate that the qualitative features of the seasonal variation in the flow in the Bab al Mandab can be explained by hydraulic processes.

a. Choice of model parameters

An analysis of historical observations in the region of the Bab al Mandab was presented by Smeed (1997). The analysis suggested that flow could be reasonably well represented by a three-layer system as illustrated in Fig. 1. Typical values of the temperature and salinity in each of the three water masses are given in Table 2 (taken from Smeed 1997). From the data presented in Smeed (1997) appropriate values of the parameters, r, $h_1(x = -\infty)$, $h_3(x = -\infty)$, $h_1(x = \infty)$, and $h_3(x = \infty)$ describing the stratification in the model reservoirs can be derived as follows

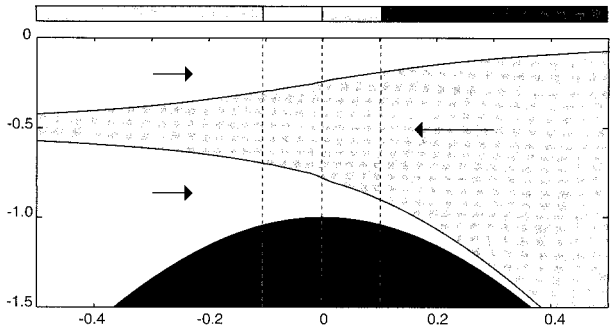

FIG. 9. Solution type [2, −2]. Parameters for the solution shown are $H_1 = 0.125$, $H_2 = 0.375$, $q_1 = 0.058$, $q_2 = -0.120$, and $q_3 = 0.062$. There are three controls (indicated by the dashed vertical lines) at $x = 0$, $x = -0.10$ and $x = +0.11$. Light shading on the bar above the plot indicates where one mode is supercritical, heavy shading indicates where both modes are supercritical.

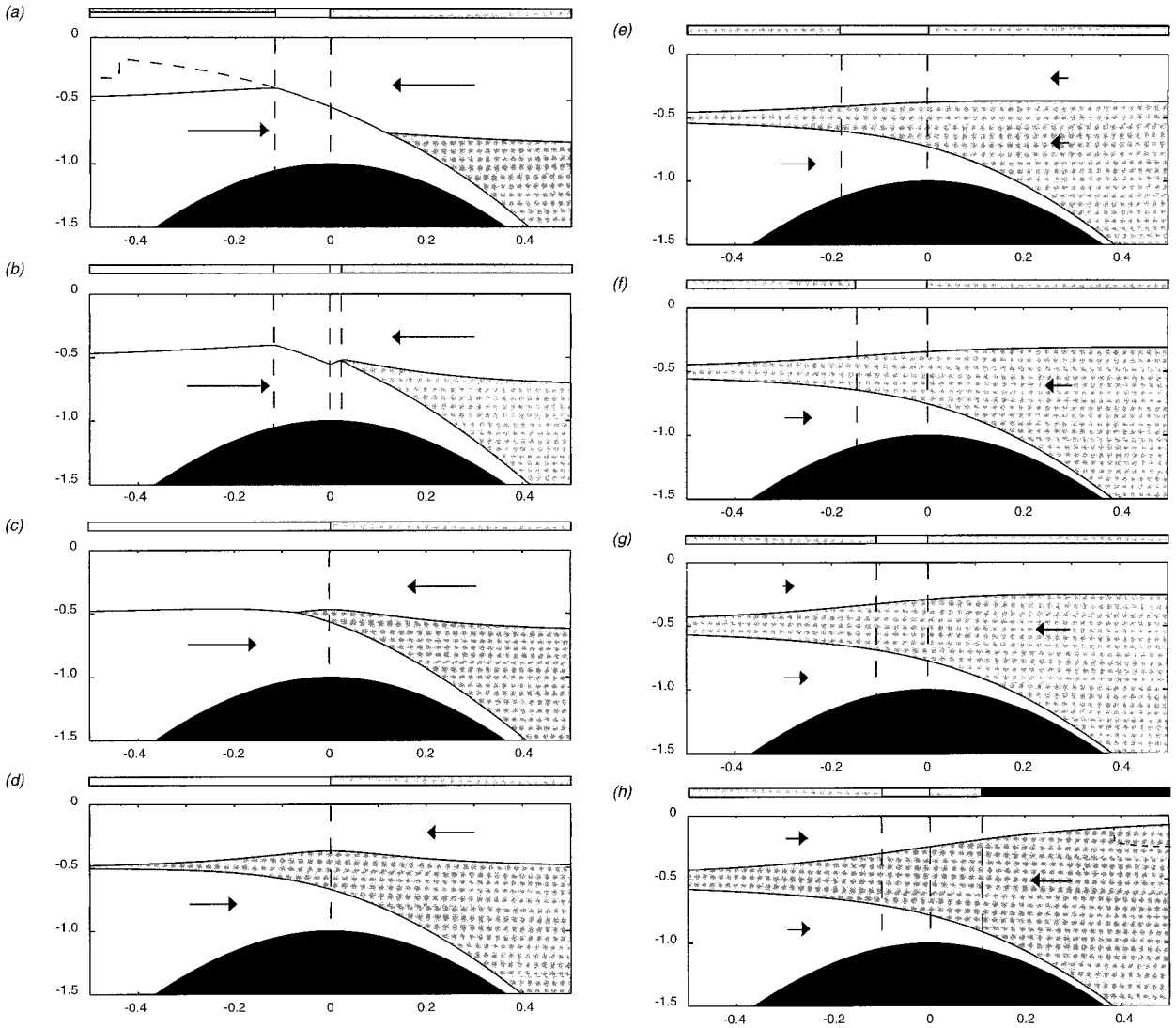

FIG. 10. Exchange flows for the case $h_1(-\infty) = 0.503H_0$, $r = 0.5$. Arrows indicate the magnitude of the flux in each layer. The depth of the upper layer in the Gulf of Aden is reduced in the sequence (a)–(h). The values of $h_1(\infty)/H_0$ are (a) 0.85, (b) 0.74, (c) 0.65, (d) 0.50, (e) 0.38, (f) 0.31, (g) 0.28, and (h) 0.00. When the depth of the upper layer is $\leq 0.25H_0$, then the flow will be of the form shown in (h) with a hydraulic jump matching the flow to the reservoir condition, as illustrated by the dashed line in (h). The locations of controls are indicated by vertical dashed lines. Light shading on the bar above the plots indicates where one mode is supercritical, heavy shading indicates where both modes are supercritical. In (a) the supercritical branch of the two-layer exchange is indicated by the dashed line. The upper bar refers to the dashed interface in (a).

In winter, r, the ratio of the density change across the upper interface to the total density change across the two interfaces, is approximately ½, heating of the surface layer in the summer increases r to approximately ⅔.

The middle layer, of Gulf of Aden intermediate water, is absent from the Red Sea in winter. In summer this layer extends well into the Red Sea, but it is assumed here that this layer is of vanishing thickness so that $h_1(x = -\infty) + h_3(x = -\infty) = H$ in both seasons (recall that H is the total depth). Note, however, that in reality the layer will have a small but finite thickness in the Red Sea during summer so that the flow is subcritical there (see section 2b). In summer the depth of the upper layer is approximately half the depth of the sill [i.e., $h_1(x = -\infty) = 0.5H_0$]. Convective mixing increase the depth of the surface layer during the winter to approximately two-thirds of the sill depth. However, the variation is small compared to the changes in the upper-layer depth in the in the Gulf of Aden.

In the Gulf of Aden, the depth of the surface layer in winter is about the same as that in the Red Sea. In summer, forced by the southwest monsoon, the interface below the surface layer rises almost to the surface. In the results presented below $h_1(x = \infty)$ is varied from 0 to H_0. The outflow of dense water from the Red Sea forms a gravity driven downslope flow in the Gulf of

TABLE 2. Approximate values of the properties of the three layers in the Babal Mandab. The reduced gravity, g', is calculated using the difference in density between the layer and the underlying layer.

Layer	Temp (°C)	Salinity (psu)	σ_θ kg m^{-3}	g′ m s^{-2}
SW–summer	32	37	22.5	0.033
SW–winter	26	37	24.5	0.014
GAIW	18	36	26.0	0.018
RSOW	22.5	40	27.9	—

Aden. For the purposes of this study it is assumed that $h_3 \to 0$ as $x \to \infty$, although in reality there may be a hydraulic jump downstream at which the lower layer depth increases again.

The bathymetry of the Bab al Mandab is complex with the minimum sill depth occurring over 100 km north of the narrowest section at Perim (see Murray and Johns 1997 for a detailed description). However, the solutions here are presented only for the idealized case of channel with a rectangular cross section, and a coincident sill and narrows.

The solutions also assume that there is no net flux through the strait. The annual mean evaporation over the Red Sea is thought to be about 2 m yr^{-1} this represents a flux through the strait of about 0.03 Sv (Sv $\equiv$ 10^6 m^3 s^{-1}) less than 10% of the exchange flux. Thus in the following calculations it is assumed that the net flux is zero.

b. *Results varying $h_1(x = \infty)$, the surface layer depth in the Gulf of Aden*

Solutions for the case $r = 0.5$, $h_1(-\infty) = 0.5$, and $0 \le h_1(\infty) \le 1$ are illustrated in Fig. 10. In Fig. 11 the fluxes in each of the three layers are shown as a function of the surface-layer depth in the Gulf of Aden reservoir.

When the upper layer is sufficiently deep in the Gulf of Aden there is no transport in the middle layer. There is a location $x = x_i$, $x_i > 0$, to the right of which there are three layers and to the left of which there are only two (e.g., Fig. 10a). To the right of x_i the upper- and lower-layers are decoupled, solutions in this part of the channel can be found by solving the two single-layer flows. To the left of x_i the flow can be solved using two-layer theory. The values of the Bernoulli constants are determined by the reservoir conditions. The flux in the upper and lower layers is that determined from two-layer theory. In the example shown, the Red Sea reservoir conditions, are those for which the two-layer flow is maximal,[5] and there is a virtual control at $x = x_v$ as well as the topographic control at $x = 0$.

As the level of the interface is raised in the Gulf of Aden the flux is unaltered but the point x_i moves toward

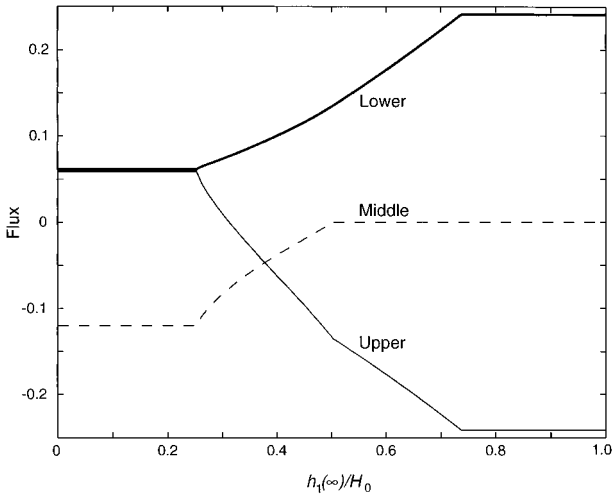

FIG. 11. Fluxes in each of the layers as a function of the depth of the upper layer in the Gulf of Aden. Other parameters are the same as in Fig. 10. Thick line = lower layer, thin line = upper layer, and dashed line = middle layer. Note that a positive flux implies flow from left to right in Fig. 10.

the sill at $x = 0$ until $x_i = 0$ [$h_1(\infty) = 0.744H_0$]. Raising the interface a little further x_i is displaced to the right again, but now the two-layer flow between $x = 0$ and $x = x_i$ is subcritical. Then a level is reached at which the single lower-layer flow is critical at x_i [$h_1(\infty) = 0.733H_0$, $x_i = 0.023$]. This case is illustrated in Fig. 10b. Raising the interface further beyond this value displaces x_i to the left and reduces the flux in the upper and lower layers, such that there is no longer a control at $x = 0$, but the single lower layer is critical at x_i For [$h_1(\infty) = 0.723H_0$], $x_i = 0$. Reducing the depth of the upper layer in the Gulf of Aden further, $x_i < 0$, but the control of the lower layer remains at $x = 0$ (Fig. 10c).

When the depth of the upper layer is the same in both reservoirs then $x_i = -\infty$ (Fig. 10d). Decreasing the depth of the upper layer in the Gulf of Aden further results in a flux in the middle layer from right to left, and a continuing reduction in the magnitude of the fluxes in the upper and lower layers (Fig. 10e). All three layers are now coupled throughout the channel. There is a control at the sill and a virtual control to the left of the sill at x_v. Using the nomenclature of section 3 this is a flow type [2, 3]. The control first appears in the Red Sea reservoir and moves towards $x = 0$ as the interface in the Gulf of Aden is raised. As noted previously the flow within the Red Sea will in reality be subcritical, that is, the middle layer will have a small but finite thickness and so a hydraulic jump is needed to connect the supercritical flow to the subcritical reservoir.

Decreasing the depth of the upper layer further the flow in the upper layer is arrested [$h_1(\infty) = 0.313H_0$, Fig. 10f] and then reversed (Fig. 10g). The flow in the middle layer reaches a maximum value when the reservoir depth is reduced to a critical value [$h_1(\infty) = 0.252H_0$]. Reducing the depth of the surface layer in

[5] Note that for the geometry used, the precise condition for maximal exchange is $h_1(-\infty) = 0.5025H_0$, and the maximal flux is $q_3 = 0.2413$.

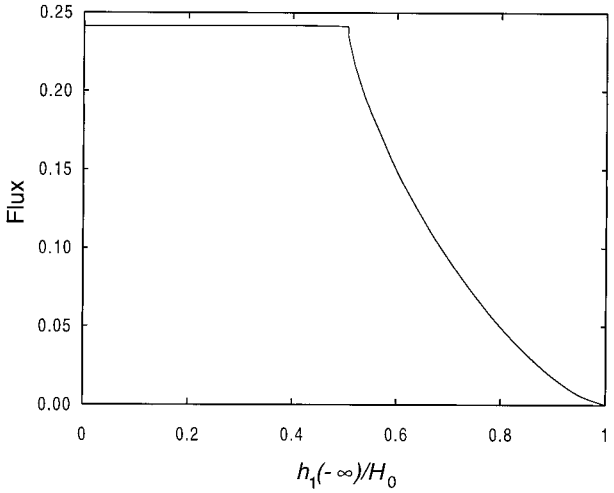

FIG. 12. Two-layer exchange flux as a function of $h_1(-\infty)$, the depth of the surface layer in the Red Sea.

reservoir further necessitates a hydraulic jump to match the reservoir conditions to the maximal solution (Fig. 10h). In this case both modes are supercritical to the right of a virtual control, at x_{v2}, on the Gulf of Aden side of the strait (flow type [2, −2]).

c. *Results varying $h_1(-\infty)$, the upper-layer depth in the Red Sea*

When the upper-layer depth in the Gulf of Aden, $h_1(\infty)$, is sufficiently deep (e.g., Fig. 10a) then the fluxes are determined by the two-layer exchange. The two-layer exchange is though dependent upon the depth of the interface in the Red Sea. For $h_1(-\infty) < 0.503H_0$ the exchange is maximal and so independent of $h_1(-\infty)$, but for $h_1(-\infty) > 0.503H_0$ the exchange is submaximal and strongly dependent upon $h_1(-\infty)$ (Fig. 12).

For $h_1(-\infty)$ a little greater than $0.503H_0$ the solutions will be quantitatively different from the case $h_1(-\infty) = 0.503H_0$, but qualitatively as $h_1(\infty)$ is decreased the flow will evolve as described in the previous section and illustrated in Fig. 10. The only difference is that the two-layer virtual control in Figs. 10a,b will not be present for $h_1(-\infty) > 0.503H_0$. For sufficiently large values of $h_1(-\infty)$ the lower layer may be arrested for some values of $h_1(\infty)$; however, these cases are not considered here.

For $h_1(-\infty) < 0.5H_0$ ($r = 0.5$) the flow can be qualitatively quite different. When the interface in the Gulf of Aden is sufficiently deep, the flux is that given by the two-layer maximal solution, but there will be a region of supercritical flow to the left of the virtual control, and a hydraulic jump connecting the supercritical flow to the subcritical reservoir. This is illustrated by the dashed solution in Fig. 10a.

The evolution of the flow as $h_1(\infty)$ is varied for $h_1(-\infty) < 0.5H_0$ is illustrated in Fig. 13 for the case

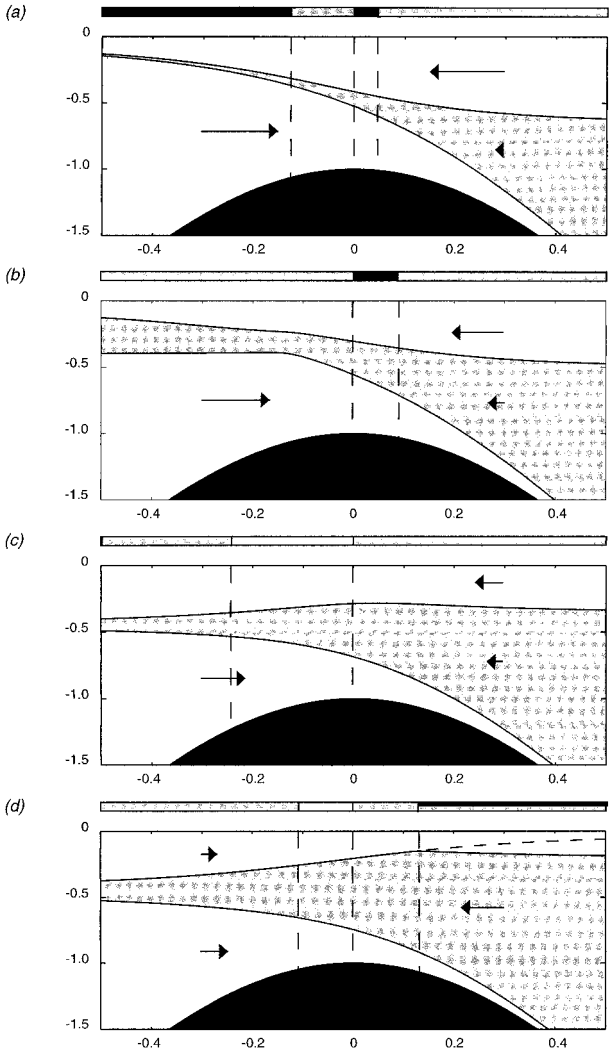

FIG. 13. Exchange flows for the case $h_1(-\infty) = 0.45H_0$, $r = 0.5$. Arrows indicate the magnitude of the flux in each layer. The depth of the upper layer in the right-hand reservoir is reduced in the sequence (a)–(d). The values of $h_1(\infty)/H_0$ are (a) 0.65, (b) 0.50, (c) 0.35, and (d) 0.20. The dashed line in (d) indicates the branch of the solution with two modes supercritical. The locations of controls are indicated by vertical dashed lines. Light shading on the bar above the plots indicates where one mode is supercritical, heavy shading indicates where both modes are supercritical. The upper bar refers to the dashed solution in (d).

$h_1(-\infty) = 0.45H_0$, $r = 0.5$. When $h_1(\infty) < 0.733H_0$ it is not possible for there to be no flux in the middle layer and for the lower layer to be controlled at $x = 0$ (as is the case in Fig. 10c) unless the upper layer is supercitical there. Instead there is control of the first mode and the flow is of the form shown in Fig. 13a (flow type [−3, 3]). There is a nonzero flux in the middle layer and a hydraulic jump is required to match the Red Sea reservoir condition to the flow. In this case there are three controls, two of these correspond to the controls in the two-layer maximal solution, but the third is introduced to the right of $x = 0$.

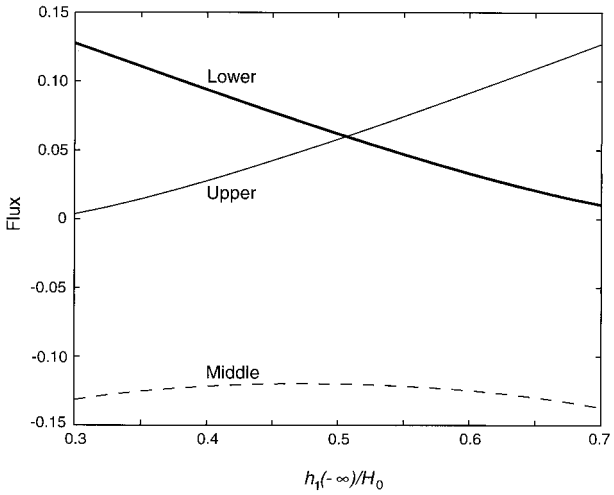

FIG. 14. Fluxes in each of the layers as a function of $h_1(-\infty)$, the depth of the upper layer in the Red Sea, for $h_3(\infty) = 0$, and $r = 0.5$. Thick line = lower layer, thin line = upper layer, and dashed line = middle layer.

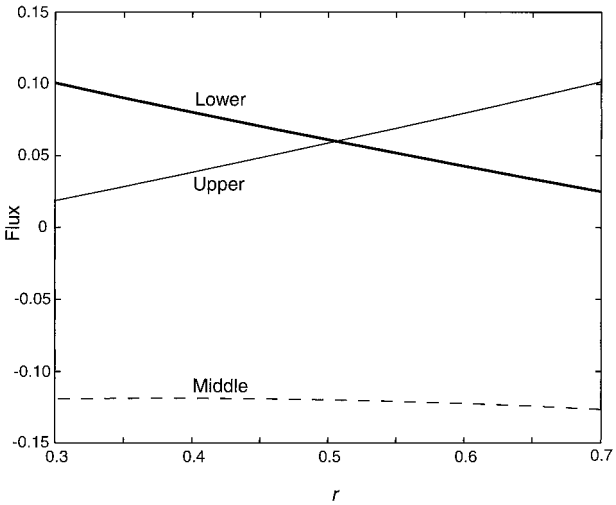

FIG. 15. Fluxes in each of the layers as a function of *r*, the ratio of the density change across the upper interface to the total density change, for $h_1(-\infty) = 0.5H_0$, and $h_3(\infty) = 0$. Thick line = lower layer, thin line = upper layer, and dashed line = middle layer.

Decreasing $h_1(\infty)$ below 0.5 H_0 (Fig. 13b) it is possible to match the lower interface to the Red Sea reservoir condition, but the flow is still controlled with respect to the first mode and a hydraulic jump is required for the upper interface. There is consequently one less virtual control. The flow is here of the type [1, 3]. For $h_1(\infty) < 0.36H_0$ the flow is controlled by the second mode only and there is a transition to the flow type [2, 3] as illustrated in Fig. 13c. The region with both modes supercritical and the virtual control to the right of the sill are lost; and a region of both modes subcritical and a virtual control are introduced to the left of the sill. Decreasing $h_1(\infty)$ further the evolution is qualitatively the same as that illustrated in Figures 10e–h. The maximal inflow of the intermediate layer is reached when $h_1(\infty) = 0.198H_0$ (Fig. 13d).

The dependence of the fluxes upon $h_1(-\infty)$ when the inflow of the intermediate layer is maximal is illustrated in Fig. 14. For $0.3 < h_1(-\infty)/H_0 < 0.7$, the flux of the intrusion in layer two does not vary greatly, however the distribution of the outflow between layers one and three does vary. Decreasing $h_1(-\infty)$ reduces the outflow in the lower layer. For values of $h_1(-\infty)$ outside the ranges illustrated in Fig. 14 either the upper or lower layer may become stagnant and there will be qualitative changes in the flow. However, an analysis of the entire parameter regime is beyond the scope of this paper.

d. Dependence of flow upon r

When the interface in the Gulf of Aden, $h_1(\infty)$, is sufficiently deep the flow is of the type illustrated in Fig. 10a, and the flux is not dependent upon *r*. Changing *r* will though affect the minimum value of $h_1(\infty)$ for which the exchange is determined by two-layer theory. It will also determine whether the flow is of the form illustrated in Fig. 10c or of the type illustrated in Fig. 13a. Flow with a subcritical upper layer, a stagnant intermediate layer and a conrolled lower layer (e.g., Fig. 10c) is only possible if $r^{0.5}h_1(-\infty) \geq (1-r)^{0.5}[H_0 - h_1(-\infty)]$, that is, if the maximal flux in the single upper is not less than the maximal flux in the single lower layer. Thus, for typical parameters appropriate for the Bab al Mandab flow like that in Fig. 13a is unlikely to occurr.

The dependence of the fluxes upon *r* when $h_1(\infty) = 0$ (i.e. when the intermediate layer inflow is maximal) is illustrated in Fig. 15. For $0.3 < r < 0.7$, the flux of the intrusion in layer two does not vary greatly, however the distribution of the outflow between layers one and three does vary. Decreasing *r* reduces the outflow in the lower layer. For values of *r* outside the ranges illustrated in Fig. 15 either the upper or lower layer may become stagnant and there will be qualitative changes in the flow.

e. Discussion

Using the data of Murray and Johns (1997), Pratt et al. (1999, 2000) have examined the criticality of the first two modes both at the Hanish Sill and the Perim narrows. It is therefore interesting to consider which of the modes is critical at each of the controls for the examples given in Figs. 10 and 13.

Displacements to the upper and lower interfaces are in phase for the first mode and out of phase for the second mode. Thus it can be shown (Lane-Serff et al 2000) that at a control it is the first mode that is critical if $F_1^2 + F_2^2 < r$. If $F_1^2 + F_2^2 > r$ then it is the second mode that is critical. At the sill, but not necessarily at the virtual controls, this implies that if the two interfaces slope in the same direction then it is the first mode that is critical, and that if they slope in opposite directions

then it is the second mode that is critical. For all of the cases presented in this paper, whenever there is only one supercritical mode, it is the second mode that is supercritical (except when there are only two layers at the control). However, the author is not aware of a proof that this is always the case.

The results presented here suggest that in the summer (e.g., Fig. 10g) only the second mode is controlled and that the first mode is everywhere subcritical, except possibly in the Gulf of Aden (Fig. 10h). For winter our results indicate that it is the first mode that is controlled (e.g., Fig. 10a).

The model results indicate that, for parameters appropriate for winter, the flux of Gulf of Aden intermediate water into the Red Sea will be zero. In the summer observation suggest that the surface layer in the Gulf of Aden is sometimes within 10 m of the sea surface. In this case the model predicts the outflow of surface water from the Red Sea and a much reduced outflow of deep water. Thus the hydraulic model is able to explain the gross characteristics of the observed seasonal variability as represented in Fig. 1.

Smeed (1997) estimated that the winter time flux was less than the two-layer maximal value. This is possible in the model if the depth of the upper layer in the Red Sea is greater than half the sill depth. The depth of the surface layer in the Gulf of Aden may also affect the flux. The observed depth of the upper layer in the Gulf of Aden is about two-thirds of the sill depth. In this case the model results indicate that the exchange flux would be less than the two-layer maximal flux, but the model also suggests that intermediate water would be present at the sill (Fig. 10c). However, the interface between the upper and lower layers in the region of the strait in winter is diffuse, and the observations do not indicate that there is any Gulf of Aden intermediate water in the strait.

There are some features in the model results that have not (so far) been reported in observations. In the summer the depth of surface layer in the Gulf of Aden is such that the model would suggest that the flow is of the form in Fig. 10h in which there is a hydraulic jump. However, it may be that stirring of the surface layer by the wind prevents the occurrence of this feature. The model also suggests that the second mode is supercritical on the Red Sea side of the strait. Pratt et al.'s (1999) analysis of Murray and Johns' (1997) data found that the flow was subcritical with respect to both modes at the Hanish Sill. This does not, however, rule out the possibility of a virtual control north of the sill.

The model is idealized and it is not surprising that there are some discrepancies. In particular the magnitude of the observed fluxes, in both summer and winter, are less than half that predicted by the model.[6] Bryden and Kinder's (1991) study of the exchange through the strait of Gibraltar showed that using a more realistic shape for the channel cross section reduced the maximal exchange by a factor of about 3. It is likely that the use of a more realistic channel cross section would significantly reduce the magnitudes of the fluxes predicted by the three-layer model.

There are a number of other processes, which are not accounted for in the model presented here including: the free surface, time dependence, and rotation. Each of these is considered briefly below.

Cromwell and Smeed (1998) have shown that the there is significant variability in sea level in the region of Bab al Mandab. Data from TOPEX/Poseidon suggest that the difference in sea level between the Red Sea and the Gulf of Aden varies by ~30 cm annually. This could be accounted for in the model by imposing a nonzero barotropic flux.

There are large tidal flows in the Bab al Mandab. Helfrich (1995) has examined the effect of oscillatory forcing on two-layer exchange flows.

Helfrich's results show that when $\gamma = (g'H_0)^{1/2}T/L$ (where T is the tidal period and L is the length of the strait) is small, then effect of the oscillatory forcing is small. Given the complex bathymetry of the strait, it is not evident how to choose the most appropriate scale for L. However, the sill at Hanish is over 100 km form the narrows at Perim, using this value for L, $\gamma \sim 1$, suggesting that the net effect of the tides is small [see Helfrich's (1995), his Fig. 9].

Pratt et al. (1999) indicate that the Rossby radii of the first two internal modes are approximately 18 and 12 km, respectively. This is comparable to the width of the strait at the Perim narrows (18 km), but the width at the Hanish sill is much greater. It seems likely that rotation will affect the exchange flow, particularly in the summer months when the flow is controlled with respect to the second mode only.

5. Conclusions

A three-layer model of hydraulically controlled exchange flows through straits has been developed. The application of the model to the Bab al Mandab has been discussed in detail; however, the model is applicable to many other strait flows. The model can represent exchange flows which are controlled with respect to either the first, second, or both internal mode(s). In contrast, two-layer models and the self-similar solution's of Engqvist (1996) can only represent control of the fastest mode.

The model is able to explain the qualitative feature of the seasonal variation of the flow in the Bab al Mandab. In particular, the reversal of the direction of flow of the surface layer and the intrusion into the Red Sea of cold intermediate water from the Gulf of Aden during the summer months can be explained by the upwelling in the Gulf of Aden forced by the southwest monsoon.

[6] Note that assuming the sill width and depth to be 18 km and 150 m, respectively, and $g' = 0.03$ m s^{-2}, then a nondimensional flux of 0.25 corresponds to a dimensional flux of about 1.4 Sv.

In the model, the intrusion of the intermediate layer is maximal when the both modes are supercritical in the Gulf of Aden. The maximal flux is though dependent upon the stratification in the Red Sea.

The magnitude of the fluxes in the model are greater than those observed. The idealized channel geometry probably accounts for most of this discrepancy, but variations in the height of the free surface and effects of rotation may also be important.

Acknowledgments. Conversations with Gregory Lane-Serff, Larry Pratt, and Peter Killworth have been very helpful in developing many of the ideas in this paper.

APPENDIX A

Solutions in the Reservoirs

Asymptotic solutions to Eqs. (11) and (12) can be derived in the limit of $b \to \infty$. There are seven possible solutions. For solution type "0," all layer depths are $O(1)$, for solution type "i" ($i = 1, 3$) layer i has thickness $O(1/b)$, and the other two layers have thickness $O(1)$, and for solution type "$-i$" ($i = 1, 3$) layer i has thickness $O(1)$ and the other two layers have depth $O(1/b)$.

Type "0"

$$y = \frac{H_1}{rh}, \tag{A1a}$$

$$z = 1 - \frac{H_2}{(1 - r)h}. \tag{A1b}$$

Type "1"

$$y^2 = \frac{q_1^2}{2b^2h^3}\frac{h}{H_1}, \tag{A2a}$$

$$z = 1 - \frac{H_2}{(1 - r)h}. \tag{A2b}$$

Type "2"

$$y = \frac{H_1 + H_2}{h}, \tag{A3a}$$

$$(1 - y - z)^2 = \frac{q_2^2}{2b^2h^3}\frac{h}{[rH_2 - (1 - r)H_1]}. \tag{A3b}$$

Type "3"

$$y = \frac{H_1}{rh}, \tag{A4a}$$

$$z^2 = \frac{q_3^2}{2b^2h^3}\frac{h}{[(1 - r)h - H_2]}. \tag{A4b}$$

Type "-1"

$$z^2 = \frac{q_3^2}{2b^2h^3}\frac{h}{[h - H_1 - H_2]}, \tag{A5a}$$

$$(1 - y - z)^2 = \frac{q_2^2}{2b^2h^2}\frac{h}{[rh - H_1]}. \tag{A5b}$$

Type "-2"

$$y^2 = \frac{q_1^2}{2b^2h^3}\frac{h}{H_1}, \tag{A6a}$$

$$z^2 = \frac{q_3^2}{2b^2h^3}\frac{h}{[(1 - r)h - H_2]}. \tag{A6b}$$

"Type -3"

$$y^2 = \frac{q_1^2}{2b^2h^3}\frac{h}{[H_1 + H_2]}, \tag{A7a}$$

$$(1 - y - z)^2 = \frac{q_2^2}{2b^2h^3}\frac{h}{H_2}. \tag{A7b}$$

Substituting these solutions into Eqs. (18) and (21) we find that

1) for solution type "0," $F_1^2, F_2^3, F_3^2 \ll 1$ and $\det(\mathbf{M}) < 0$;
2) for solution type "i," ($i = 1, 3$), $F_i^2 = O(bh^{3/2}) \gg 1$, $F_j^2 \ll 1$ ($j \neq i$), and $\det(\mathbf{M}) > 0$; and
3) for solution type "$-i$," ($i = 1, 3$), $F_i^2 \ll 1$, $F_j^2 = O(bh^{3/2}) \gg 1$ ($j \neq i$), and $\det(\mathbf{M}) < 0$.

APPENDIX B

Numerical Solutions

For the examples given in this paper the channel geometry is described by

$$h(x) = h_m + (1 - h_m)e^{-x^2} \tag{B1}$$

$$b(x) = b_m + (1 - b_m)e^{-x^2}, \tag{B2}$$

and the maximum nondimensional depth and width, h_m and b_m, were both set equal to 5.

For given values of the fluxes and the Bernoulli constants, solutions for y and z as a function of x were obtained as follows. Given values $y(x)$, $z(x)$ estimates of $y(x + \delta x)$, $z(x + \delta x)$ were calculated using a forward difference form of Eq. (16), these estimates were then used as an initial guess for a numerical procedure to find solutions to eqs. (11) and (12) at $x + \delta x$. The procedures used to obtain the solutions described in sections 3 and 4 are outlined below.

a. Subcritical flow in both reservoirs

Solutions that are everywhere subcritical are symmetric about $x = 0$ and were evaluated as follows. Given the values of the Bernoulli constants and the fluxes, the

upstream solution was evaluated using the analytical expression for solution type ''0'' (A1), Eq. (16) was then integrated up to $x = 0$.

To find the boundary of the area in the (q_1, q_3) plane for which subcritical solutions are possible (Fig. 4), a binary search was used to find values of the fluxes for which $\det(\mathbf{M}) = 0$ at $x = 0$.

b. Both modes subcritical upstream, one mode supercritical downstream

The procedure in *a* above was repeated to find the lines in the (q_1, q_3) plane on which $\det(\mathbf{M}) = 0$ at $x = 0$ for each of the reservoir solutions 0, 1, 2, and 3. The values of the fluxes for which the upstream and downstream solutions matched at $x = 0$ were then determined.

c. One mode supercritical upstream, one mode supercritical downstream

The values of the Bernoulli functions are determined by the reservoir conditions. The fluxes were determined by solving the seven following equations

(11), (12), and (20) at $x = 0$;

(11), (12), (20), and (22) at $x = x_v$,

for the seven following variables:

$$q_1,\ q_2,\ x_v,\ y(0),\ z(0),\ y(x_v), \text{ and } z(x_v).$$

Once the fluxes were determined the complete solution $[y(x), z(x)]$ was obtained by integrating along the channel starting from the analytic solutions in the reservoirs as described above

d. Two modes subcritical upstream, two modes supercritical downstream

The method in section c of appendix B above was also used for this case.

e. One mode supercritical downstream two modes supercritical upstream

Only one of the Bernoulli constants is determined by the reservoir conditions. The other constant and the fluxes were determined by solving the 11 following equations.[A1]

(11), (12), and (20) at $x = 0$;

(11), (12), (20), and (22) at $x = x_v$;

(11), (12), (20), and (22) at $x = x_{v2}$,

for the following 11 variables:

$$L(H_i),\ q_1,\ q_2,\ x_v,\ x_{v2},\ y(0),\ z(0),\ y(x_v),\ z(x_v),$$
$$y(x_{v2}), \text{ and } z(x_{v2}).$$

For flow type [2, −2] (e.g., Fig. 10h) for which $H_1 + H_2$ is set on the Red Sea side of the sill, $L(H_i) = H_1 - H_2$. For flow type [−3, 3] (e.g., Fig. 13a) for which H_1 is set on the Gulf of Aden side of the sill, $L(H_i) = H_2$. Once the fluxes were determined, the complete solution $[y(x), z(x)]$ was obtained by integrating along the channel starting from the analytic solutions in the reservoirs as described above.

REFERENCES

Armi, L., 1986: The hydraulics of two flowing layers with different densities. *J. Fluid Mech.,* **163,** 27–58.

——, and D. M. Farmer, 1986: Maximal two-layer exchange through a contraction with barotropic net flow. *J. Fluid Mech.,* **164,** 27–51.

——, and R. Williams, 1993: The hydraulics of a stratifed fluid flowing through a contraction. *J. Fluid Mech.,* **251,** 355–375.

Baines, P. G., 1987: Upstream blocking and airflow over mountains. *Annu. Rev. Fluid Mech.,* **19,** 75–97.

——, 1988: A general method for determining upstream effects in stratified flow of finite depth over long two-dimensional obstacles. *J. Fluid Mech.,* **188,** 1–22.

——, 1995: *Topographic Effects in Stratified Flows.* Cambridge University Press, 482 pp.

Bormans, M., and C. Garrett, 1989: The effects of nonrectangular cross section, friction, and barotropic fluctuations on exchange through the Strait of Gibraltar. *J. Phys. Oceanogr.,* **19,** 1543–1557.

Bryden, H. L., and T. H. Kinder, 1991: Steady two-layer exchange through the Strait of Gibraltar. *Deep-Sea Res.,* **38,** 5445–5463.

——, J. Candella, and T. H. Kinder, 1994: Exchange through the Strait of Gibraltar. *Progress in Oceanography,* Vol. 33, Pergamon, 201–248.

Cromwell, D., and D. A. Smeed, 1998: Altimetric observations of sea level cycles near the Strait of Bab al Mandab. *Int. J. Remote Sens.,* **19,** 1561–1578.

Dalziel, S. B., 1990: Rotating two-layer sill flows. *The Physical Oceanography of Sea Straits,* L. J. Pratt, Ed., Kluwer Academic, 343–371.

——, 1991: Two-layer hydraulics: A functional approach. *J. Fluid Mech.,* **223,** 135–163.

——, 1992: Maximal exchange in channels with nonrectangular cross sections. *J. Phys. Oceanogr.,* **22,** 1188–1206.

Denton, R. A., 1990: Classification of unidirectional three-layer flow over a bump. *J. Hydraul. Res.,* **28,** 215–223.

Engqvist, A., 1996: Self-similar multi-layer exchange flow through a contraction. *J. Fluid Mech.,* **328,** 49–66.

Farmer, D. M., and L. Armi, 1986: Maximal two-layer exchange over a sill and through the combination of a sill and contraction with barotropic flow. *J. Fluid Mech.,* **164,** 53–78.

——, and ——, 1988: The flow of Mediterranean water through the Strait of Gibraltar. *Progress in Oceanography,* Vol. 27, Pergamon, 1–41.

Gill, A. E., 1977: The hydraulics of rotating channel flow. *J. Fluid Mech.,* **80,** 641–671.

Helfrich, K. R., 1995: Time-dependent two-layer hydraulic exchange flows. *J. Phys. Oceanogr.,* **25,** 359–373.

Hogg, N. G., 1983: Hydraulic control and flow separation in a multilayered fluid with applications to the Vema Channel. *J. Phys. Oceanogr.,* **13,** 695–708.

Imberger, J., and J. C. Patterson, 1990: Physical limnology. *Adv. Appl. Mech.,* **27,** 303–475.

Killworth, P. D., 1992: On hydraulic control in a stratified fluid. *J. Fluid Mech.,* **237,** 605–626.

Lane-Serff, G. F., D. A. Smeed, and C. R. Postlethwaite, 2000: Multilayer hydraulic exchange flows. *J. Fluid Mech.,* in press.

Maillard, C., and G. Soliman, 1986: Hydrography of the Red Sea

and exchanges with the Indian Ocean in summer. *Oceanol. Acta,* **9,** 249–269.
Murray, S. P., and W. Johns, 1997: Direct observations of seasonal exchange through the Bab el Mandab Strait. *Geophys. Res. Lett.,* **24,** 2557–2560.
Patzert, W. C., 1974: Wind induced reversal in the Red Sea circulation. *Deep-Sea Res.,* **21,** 109–121.
Pratt, L. J., and P. A. Lundberg, 1991: Hydraulics of rotating strait and sill flows. *Annu. Rev. Fluid Mech.,* **23,** 81–106.
——, W. Johns, S. P. Murray, and K. Katsumata, 1999: Hydraulic interpretation of direct velocity measurements in the Bab al Mandab. *J. Phys. Oceanogr.,* **29,** 2769–2784.
——, H. E. Deese, S. P. Murray, and W. Johns, 2000: Continuous dynamical modes in straits having arbitrary cross sections, with applications to the Bab al Mandab. *J. Phys. Oceanogr.,* **30,** 2515–2534.
Smeed, D., 1997: Seasonal variation of the flow in the Strait of Bab al Mandab. *Oceanol. Acta,* **20,** 773–781.